Available online at www.sciencedirect.com
ScienceDirect
Journal of Non-Crystalline Solids 352 (2006) 3739–3743
JOURNAL OF NON-CRYSTALLINE SOLIDS
www.elsevier.com/locate/jnoncrysol

Manufacturing of porous niobium phosphate glasses

C.R. Rambo [a,*], L. Ghussn [b], F.F. Sene [b], J.R. Martinelli [b]

[a] *Federal University of Santa Catarina – UFSC, P.O. Box 476, 88040-900 Florianópolis/SC, Brazil*
[b] *Energy and Nuclear Research Institute, Center of Materials Science and Technology, Av. Lineu Prestes, 2242, Cidade Universitária, 05588-900 Sao Paulo, SP, Brazil*

Available online 4 August 2006

Abstract

Niobium phosphate glasses with composition $33P_2O_5 \cdot 27K_2O \cdot 40Nb_2O_5$ are usually very stable with regard to crystallization resistance, with a relatively high glass transition temperature ($T_g \sim 750$ °C), and are potentially suitable for nuclear waste immobilization. Porous niobium phosphate glasses were prepared by the replication method. The porous glasses were produced via the dip-coating of an aqueous slurry containing 20 wt% powdered glass into commercial polyurethane foams. The infiltrated foams were oxidized at 600 °C for 30 min to decompose the polymeric chains and to burn out the carbon, leading to a fragile glass skeleton. Subsequent heating above the glass transition temperature in the range of 780–790 °C for 1 h, finally resulted in mechanically stable glass foams, which maintained the original interconnected pore structure of the polyurethane foam. The struts showed the neck formation between particles, evidencing the initial stage of sintering. The open and interconnected porosity of the glassy foams lies in the range of 85–90 vol.%. It was concluded that porous niobium phosphate glasses are potential candidates for immobilizing liquid nuclear waste.

Keywords: Porosity; Nuclear and chemical wastes; Phosphates

1. Introduction

In recent years, interest in materials with cellular structures, such as foams and reticulated and biomorphic materials, has increased due to their specific properties, such as low density (<1.0 g/cm^3), low thermal conductivity, thermal stability at temperatures up to 1500 °C, high surface area, and high permeability [1–4]. Foams are a special class of porous materials comprised of large voids (open or closed cells), with linear dimensions approximately ranging from a few micrometers to few millimeters (10 μm–5 mm), and exhibit geometries similar to that of a tetrakaidecahedron [5,6]. These properties make foams suitable for a wide range of technological applications, including catalyst supports, filters for molten-metals and hot gases, thermal insulators, refractory linings, and biomaterials [7–9]. Various processing routes have been proposed for the production of ceramic foams, including the polymeric sponge method [10,11], direct foaming and foaming agents [12–14] and the space holder method [15]. The fabrication method determines the range of porosity, the pore size distribution, and the pore morphology.

The polymeric sponge method [11], or replication method, is a simple, inexpensive and versatile way of producing ceramic foams. This method consists of the impregnation of a polymeric sponge with slurries containing appropriate binders, followed by a heat-treatment to burn out the organic template (sponge) and to sinter the remaining skeleton. Among a wide range of ceramics that can be made by this method, zirconia, silicon carbide and alumina are the most usual [8,10,14,16]. However, only few studies have dealt with the production of cellular glass–ceramics or glasses [17–21].

Phosphate glasses have received considerable attention in the past few years due to the possibility of producing new glass compositions with high chemical and thermodynamic stability. Phosphate glasses can be used, among other applications, in the hermetic sealing of metallic and ceramic materials [22], optical applications [23] and nuclear waste immobilization [24]. However, phosphate glasses are

* Corresponding author. Tel.: +55 48 3331 9713; fax: +55 48 3331 9687.
E-mail address: rambo@enq.ufsc.br (C.R. Rambo).

0022-3093/$ - see front matter © 2006 Elsevier B.V. All rights reserved.
doi:10.1016/j.jnoncrysol.2006.03.104

known to have low resistance to humid environments. The addition of iron has increased the chemical durability of these glasses enabling their use as nuclear wasteforms [25]. When Fe is substituted by Nb, phosphate glasses with leaching rates, in aqueous media at 90 °C, in the order of 10^{-6} g cm^{-2} d^{-1} are obtained [26,27]. The improvement of chemical stability has stimulated the application of phosphate glasses in several fields of materials science, including optical and laser applications [28,29].

This paper reports the manufacturing and characterization of highly porous niobium phosphate glass foams by dip-coating. The porous glasses were physically characterized and analyzed in terms of their macro and microstructures in order to evaluate their potential application in nuclear waste immobilization.

2. Experimental procedures

A niobium phosphate glass was obtained by melting mixtures of inorganic precursors (reagent grade) in an electrical furnace at 1350 °C for 1 h in alumina crucibles. The glass composition was $33P_2O_5 \cdot 27K_2O \cdot 40Nb_2O_5$ in mol% (hereafter named as Nb40). The raw materials were: Nb_2O_5 (supplied by Companhia Brasileira de Metalurgia e Mineração, CBMM, Brazil), $NH_4H_2PO_4$ (Merk) and KOH (Cicarelli). The liquid was cast in a stainless steel mold. After cooling, the Nb40 glass was milled for 3 h to achieve particles with sizes smaller than ~45 μm.

The phosphate glass containing 40 mol% NB_2O_5 was chosen based on previous studies reported elsewhere [26,30], due to its high chemical resistance in aqueous media. The addition of niobium oxide in phosphate glasses improves its chemical durability. This is associated with the O–Nb–O and mixed O–P–O–Nb–O– chain bonds.

Aqueous slurries containing 20 wt% of glass powder and 0.15 wt% of carboxymethyl cellulose (CMC), used as a binder, were prepared for the dip-coating of the foams. Commercial polyurethane foams with a monomodal pore size distribution (55 ± 5 pores per inch) and porosity of 95% ± 1% were used as templates. The polymeric foams were cut in pieces of approximately $30 \times 25 \times 20$ mm^3 and immersed in the Nb40 parent glass slurry for 2–3 s. The impregnated foams were lightly compressed to remove the excess slurry.

Due to the relatively poor wettability of the polyurethane [31], the relative low viscosity of the aqueous slurry causes a rapid flow after impregnation, which prevents the formation of a homogeneous coating layer. Therefore, a drying stage after coating was not adopted in order to avoid loss of the material from the foam structure. The as-infiltrated foams were then treated at 600 °C for 30 min to decompose the polymeric chains and to burn out the carbon, leading to a fragile glass skeleton. Subsequent heating above the glass transition temperature (T_g), in the range of 740–780 °C for 1 h finally resulted in mechanically stable foams.

Thermogravimetric analysis (TGA, Du Pont Instruments, 951 Thermo) of the polymeric foam was performed in air with a heating rate of 10 °C/min in order to establish an appropriate heat treatment. Differential thermal analysis (DTA, Netzsch, STA 409) of the Nb40-glass powder was performed in air at a heating rate of 15 °C/min to determine the typical Nb40-glass temperatures. X-ray diffraction (XRD, Diffrac 500, Siemens AG, Mannheim, Germany) with CuKα radiation was used to identify the phases of the final product. The strut density was determined by He-pycnometer (AccuPyc 1330, Micromeritics, Norcross, GA). The open porosity was derived from the relation between the strut density and the geometrical density. Fourier Transformed Infrared Spectroscopy (FT-IR, Thermo Nicolet, Nexus, 670) was performed using glass powder dispersed in dehydrated KBr pellets and also with a thin piece of glass (monolithic).

3. Results

The TGA curve of the polyurethane foam revealed two weight loss stages. The first one, between 250 and 400 °C, which corresponds to the decomposition of the polymer, resulted in an accentuated weight loss. The second stage, between 400 and 600 °C, is attributed to the oxidation of carbon derived from the decomposition of the polymers of the foam [18]. The TGA result allows the selection of the optimized thermal cycle for the decomposition of the foams.

3.1. Nb-glass characterization

The characteristic temperatures of Nb40 glasses have previously been reported elsewhere [26]. A T_g of 715 °C and a crystallization temperature of 944 °C were reported. However, a slight difference in the composition was adopted in this study to improve the thermal stability of the Nb40 glasses. The amount of P_2O_5 was increased whilst the amount of K_2O was decreased, which resulted in an increase in both transition and crystallization temperatures. The glass transition temperature determined by the DTA curve (shown in Fig. 1) is 783 ± 5 °C and the crystallization peak is located at 990 ± 5 °C. By knowing the tran-

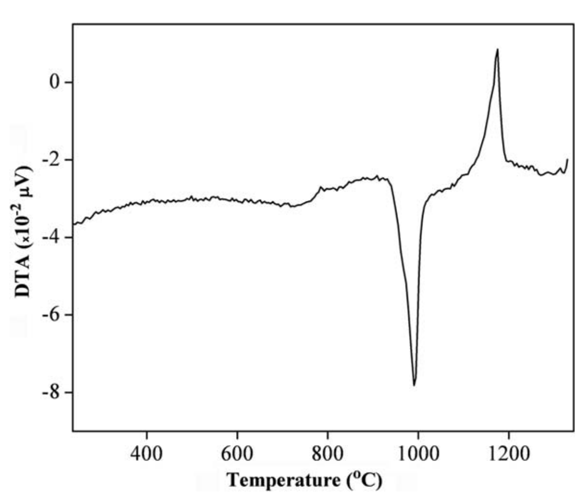

Fig. 1. DTA curve of the Nb40 parent glass.

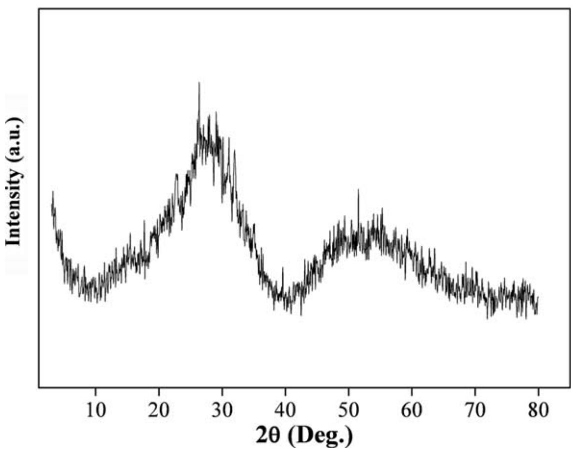

Fig. 2. X-ray diffraction pattern of the powdered Nb40 glass foam.

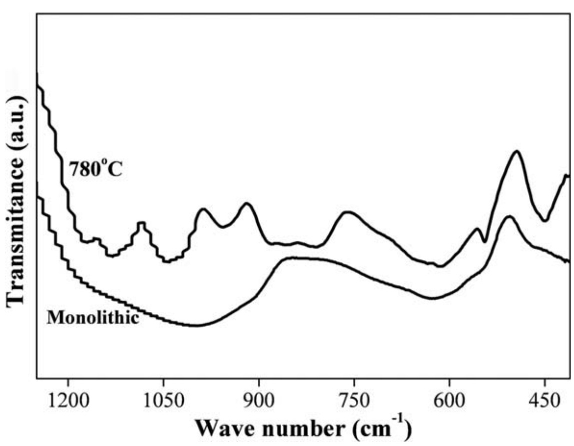

Fig. 3. FTIR spectra of the powder (treated at 780 °C for 36 h) and the monolithic Nb40 parent glass.

sition temperature, it is possible to optimize the processing conditions for producing the glass foams.

Fig. 2 shows the X-ray diffraction pattern of the powdered foam after the thermal treatment. The glass foam consists of an amorphous phase, characterized by two halos centered in $2\theta = 30°$ and 55°, respectively, and its XRD pattern shows the absence of sharp peaks that could be related to crystalline phases. Surface crystallization could not be detected by XRD, which typically detects crystalline phases in concentrations higher than 1.5 wt%.

The FTIR spectra of the Nb40 glass (powder and monolithic) are shown in Fig. 3. The powder was heat treated at 780 °C for 36 h to promote crystallization. The monolithic glass was not crystallized and exhibits no defined bands due to the absence of periodicity, characteristic of an amorphous material. The glass powder bands exhibited smaller widths compared to those of the monolithic glass with no differences in their positions, which suggests that after heat treatment, the sample retained its local structure [32]. Most of the IR bands have been previously identified. IR bands located at 1228, 990, and 910 cm^{-1} have been assigned to P═O stretching, the $(PO_4)^{3-}$ ionic group and P–O–H bending, respectively [33,34]. Bands located at 740–714 cm^{-1} are assigned to P–O–P stretching vibration. Bands located at 584– 630 cm^{-1} are assigned to O–Nb vibration. The bands at 530–510 cm^{-1} are related to P–O–P stretching vibrations, or harmonics of bending O–P–O and O═P–O bonding [33,34].

3.2. Foam characterization

Fig. 4 shows optical micrographs obtained by optical microscope, evidencing visual aspects of the surface of the Nb40 glass foam. A surface characteristic of a foam structure is clearly seen in Fig. 4(a). In Fig. 4(b) a slightly reflective surface characteristic of a glassy surface can be seen. The pores are uniformly distributed on the glass surface. The open, interconnected porosity of the foams lies in the range of 85–90 vol.%, with an apparent density of 0.4–0.5 g/cm^3.

Fig. 5 shows the SEM micrographs of the Nb40-glass foam. The glass foam exhibits a relative non-homogeneity in pore morphology, characterized by cell wall discontinuity on the surface (Fig. 5(a)). Large voids (up to 1 mm) can be seen within the small pores (0.2–0.5 mm), forming a mixed pore network. Additionally, the pores of the foam are mostly open and interconnected.

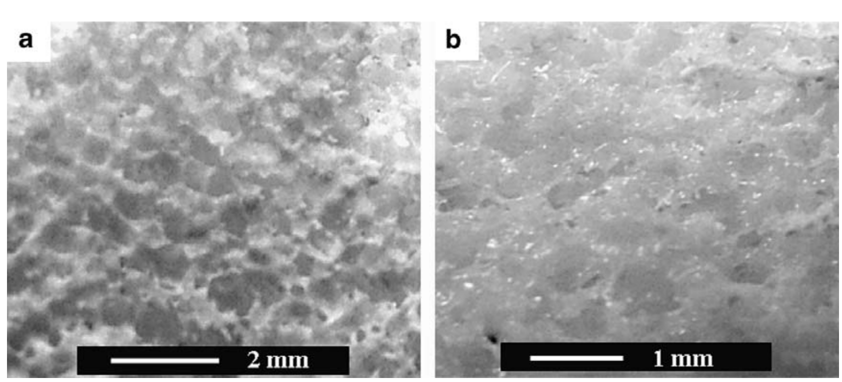

Fig. 4. Optical photograph of the surface of the Nb40 glass foam.

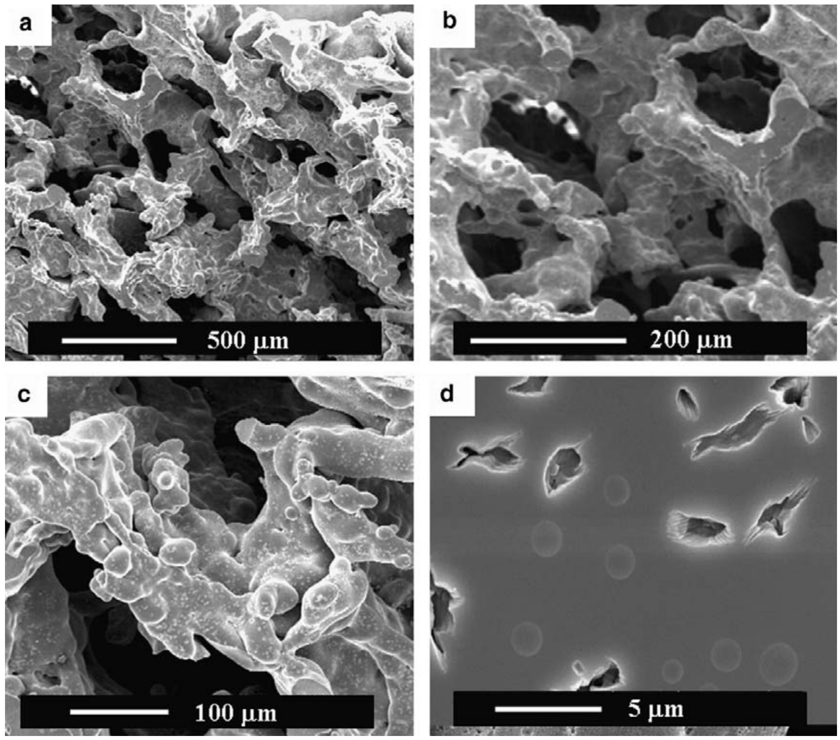

Fig. 5. SEM micrographs of the glass foam. (a)–(d) Show different magnitudes of the same sample.

4. Discussion

By heating the material above the T_g, a significant deformation of the original polyurethane foam structure is observed, which explains the observed elongated pore morphology in Fig. 5(a) and (b). The struts showed the neck formation between particles, evidencing the initial stage of sintering (Fig. 5(c)). Surface crystallization also occurred, evidenced by the presence of small crystals on the strut surface (Fig. 5(d)). The crystal nuclei exhibit sizes of approximately 2–5 μm and are homogeneously distributed on the surface of the struts with a density of approximately 1.1×10^7 nuclei/mm^2, which is one order of magnitude lower than the density reported by Ghussn et al. [35]. Surface crystallization is less critical than volume crystallization with regard to the effects caused by possible defects arising from the devitrification process if the glass foam is intended to be used for nuclear waste immobilization. However, a compromise between the densification and crystallization temperatures must be found without losing the mechanical strength of the foams.

5. Conclusions

Niobium phosphate glass foams with interconnected pores and high porosity (90–95%) were obtained by the polymeric foam method. This method allowed the partial replication of the original polyurethane foam structure. The glass foams consist mainly of an amorphous phase. Dense struts with minor surface crystallization were obtained by sintering the parent glass particles. Niobium phosphate glasses with controlled porosity can be used as scaffolds in biomedical applications, filters and porous hosts for liquid nuclear waste after sealing.

Acknowledgements

C.R. Rambo and L. Ghussn thank CNPq-Brazil for granting a scholarship. Companhia Brasileira de Metalurgia e Mineracao (CBMM-Brazil) is also acknowledged for supplying Nb_2O_5. The authors are thankful to J.F. Liberati for helping with the optical microscopy analyses.

References

[1] P. Colombo, E. Bernardo, Compôs. Sci. Technol. 63 (2003) 2353.
[2] M.D.M. Innocentini, A.R.F. Pardo, B.A. Menegazzo, L.R.M. Bittencourt, R.P. Rettore, V.C. Pandolfelli, J. Am. Ceram. Soc. 85 (2002) 1517.
[3] C.R. Rambo, H. Sieber, Adv. Mater. 17 (2005) 1088.
[4] P. Ciambelli, V. Palma, P. Russo, S. Vaccaro, Catal. Today 75 (2002) 471.
[5] L.J. Gibson, M.F. Ashby, Cellular Solids: Structure and Properties. Pergamon Press, New York, 1988.
[6] L.J. Gibson, J. Biomech. 38 (2005) 377.
[7] P. Sepulveda, Am. Ceram. Soc. Bull. 76 (1997) 61.
[8] R. Brezny, D.J. Green, In Materials Science and Technology, in: R.W. Cahn, P. Haasen, E.J. Kramer (Eds.), Structure and Properties of Ceramics, 11, VCH, Germany, 1992, p. 467.
[9] C.R. Rambo, F.A. Mueller, L. Mueller, H. Sieber, I. Hofmann, P. Greil, Mater. Sci. Eng. C 26 (2006) 92.
[10] L. Montanaro, Y. Jorand, G. Fantozzi, A. Negro, J. Eur. Ceram. Soc. 18 (1998) 1339.

[11] K. Schwartzwalder, A.V. Somers, US Pat. No. 3 090 094, May 21, 1963.
[12] J. Saggio-Woyansky, C.E. Scottetal, Am. Ceram. Soc. Bull. 71 (1992) 1674.
[13] P. Sepulveda, J.G.P. Binner, J. Eur. Ceram. Soc.19 (1999) 2059.
[14] J. Zeschky, T. Höfner, C. Arnold, R. Weißmann, D. Bahloul-Hourlier, M. Scheffler, P. Greil, Acta Mater. 53 (2005) 927.
[15] H.X. Peng, Z. Fan, J.R.G. Evans, J.J.C. Busfield, J. Eur. Ceram. Soc. 20 (2000) 807.
[16] T.J. Fiztgerald, A. Mortensen, V.J. Michaud, J. Mater. Sci. 30 (1995) 1037.
[17] N.M. Bobkova, N.I. Zayatz, T.V. Kolontaeva, G.N. Punko, G.B. Zakharevich, Glass Ceram. 57 (2000) 412.
[18] E. Sousa, C.B. Silveira, T. Fey, P. Greil, D. Hotza, A.P.N. Oliveira, Adv. Appl. Ceram. 104 (2005) 22.
[19] A.R. Boccaccini, J. Porous Mat. 6 (1999) 369.
[20] Young-Wook Him, Shin-Han Kim, Hai-Doo Kim, Chul B. Park, J. Mater. Sci. 39 (2004) 5647.
[21] Lev D. Gelb, K.E. Gubbins, Langmuir 14 (1998) 2097.
[22] T.L. White, C.D. Bostick, C.T. Lson C.R. Schaich, Workshop, San Antonio, TX, USA, 5–6 November, 1995.
[23] B.C. Sales, L.A. Boatner, J. Am. Ceram. Soc. 70 (1987) 615.
[24] B.C. Sales, L.A. Boatner, J. Non-Cryst. Solids 79 (1986) 83.
[25] D.E. Day, Z. Wu, C.S. Ray, P.R. Hrma, J. Non-Cryst. Solids 241 (1998) 1.
[26] L. Ghussn, J.R. Martinelli, J. Mater. Sci. 39 (2004) 1371.
[27] F.F. Sene, PhD thesis, IPEN - São Paulo, Brazil, 2002.
[28] I.O. Mazali, L.C. Barbosa, O.L. Alves, J. Mater. Sci. 39 (2004) 1987.
[29] F.F. Sene, J.R. Martinelli, L. Gomes, J. Non-Cryst. Solids 348 (2004) 63.
[30] L. Ghussn, PhD thesis, IPEN - São Paulo, Brazil, 2005.
[31] S.K. Koh, J.S. Cho, K.H. Kim, S. Han, Y.W. Beag, J. Adhes. Sci. Technol. 16 (2002) 129.
[32] S.T. Reis, D.L.A. Faria, J.R. Martinelli, W.M. Pontuschka, D.E. Day, C.S.M. Partiti, J. Non-Cryst. Solids 304 (2002) 188.
[33] C. Dayanand, G. Bhikshamaiah, V. Jayatyagaraju, M. Salagram, A.S.R. Krishna Murthy, J. Mater. Sci. 31 (1996) 1945.
[34] F. F Sene, J.R. Martinelli, L. Gomes, J.Non-Cryst. Solids 348 (2004) 30.
[35] L. Ghussn, M.O. Prado, D.O. Russo, J.R. Martinelli, in: 3rd Brazil MRS Meeting, October 10–13, 2004, Foz do Iguaçu, Brazil.